

PROCEEDINGS OF VIPIMAGE 2013 – IV ECCOMAS THEMATIC CONFERENCE ON
COMPUTATIONAL VISION AND MEDICAL IMAGE PROCESSING, FUNCHAL, PORTUGAL, 14–16
OCTOBER 2013

Computational Vision and Medical Image Processing IV

Editors

João Manuel R.S. Tavares & R.M. Natal Jorge

Departamento de Engenharia, Universidade do Porto, Porto, Portugal



CRC Press

Taylor & Francis Group

Boca Raton London New York Leiden

CRC Press is an imprint of the
Taylor & Francis Group, an **informa** business

A BALKEMA BOOK

CRC Press/Balkema is an imprint of the Taylor & Francis Group, an informa business

© 2014 Taylor & Francis Group, London, UK

Typeset by V Publishing Solutions Pvt Ltd., Chennai, India

Printed and bound in Great Britain by CPI Group (UK) Ltd, Croydon, CR0 4YY

All rights reserved. No part of this publication or the information contained herein may be reproduced, stored in a retrieval system, or transmitted in any form or by any means, electronic, mechanical, by photocopying, recording or otherwise, without written prior permission from the publisher.

Although all care is taken to ensure integrity and the quality of this publication and the information herein, no responsibility is assumed by the publishers nor the author for any damage to the property or persons as a result of operation or use of this publication and/or the information contained herein.

Published by: CRC Press/Balkema

P.O. Box 11320, 2301 EH Leiden, The Netherlands

e-mail: Pub.NL@taylorandfrancis.com

www.crcpress.com – www.taylorandfrancis.com

ISBN: 978-1-138-00081-0 (Hbk)

ISBN: 978-1-135-81292-2 (eBook PDF)

Table of contents

Preface	ix
Acknowledgements	xi
Invited lecturers	xiii
Thematic sessions	xv
Scientific committee	xvii

Invited lectures

Machine learning meets medical imaging: Learning and discovery of clinically useful information from images <i>D. Rueckert, R. Wolz & P. Aljabar</i>	3
Seeing and understanding people <i>R. Bowden</i>	9

Contributed papers

On the strain–line patterns in a real human left ventricle <i>S. Gabriele, L. Teresi, V. Varano, A. Evangelista, P. Nardinocchi, P.E. Puddu & C. Torromeo</i>	19
MR-T2-weighted signal intensity: A new imaging marker of prostate cancer aggressiveness <i>V. Giannini, A. Vignati, S. Mirasole, F. Russo, D. Regge, S. Mazzetti, C. Bracco & M. Stasi</i>	25
Dimensionality reduction through LDA and bag-of-features applied to image retrieval <i>R.E.G. Valenzuela, H. Pedrini & W.R. Schwartz</i>	31
Prediction-assisted moving objects tracking in severe occlusions and background clutters <i>M. Ahmed, Y. Ahn & J. Choi</i>	39
Scale and orientation adaptive histogram-based object tracking in video sequences <i>Z. Ren, Y. Ahn & J. Choi</i>	45
Wavelet approach for studying motor strategy patterns of diabetic neuropathic individuals in gait cycle <i>C.G.F. Pachi, H.A. Weiderpass, J.F. Yamamoto, I.C.N. Sacco, A. Hamamoto & A.N. Onodera</i>	51
Fully discrete, nonlocal models for image processing: Properties and applications <i>E. Cuesta & A. Durán</i>	55
Image smoothing using the Perona-Malik equation with a new estimation method of the contrast parameter <i>M. Borroto-Fernández, A. León-Mecías & M. González-Hidalgo</i>	59
Speckle ultrasound image filtering: Performance analysis and comparison <i>R. Rosa & F.C. Monteiro</i>	65
A study of the complexity of respiratory signals during wake and sleep <i>C.H. González & G.A. Sánchez</i>	71
Model-based extraction of input and organ functions in dynamic medical imaging <i>O. Tichý, V. Šmídl & M. Šámal</i>	75

A study on clustering for colour image quantisation <i>H. Palus & M. Frackiewicz</i>	81
Sparse and robust signal reconstruction algorithm <i>S.V.B. Jardim</i>	87
An empirical study of algebraic-reconstruction techniques <i>E.M. Kazemi & N.S. Nedialkov</i>	93
Fast soft switching impulsive noise removal in color images <i>B. Smolka</i>	99
Analysis of the retinal nerve fiber layer texture related to the thickness measured by optical coherence tomography <i>J. Odstrcilik, R. Kolar, R.P. Tornow, A. Budai, J. Jan, P. Mackova & M. Vodakova</i>	105
A selective denoising method to remove speckle noise <i>A.F. de Araujo, J.M.R.S. Tavares & C.E. Constantinou</i>	111
Registration of the long-term autofluorescence retinal images taken from glaucomatic patients <i>R. Kolar, J. Odstrcilik, R. Laemmer & P. Mackova</i>	115
Simplified and labelled bone model reconstruction for interactive environments <i>R. Pulido, J.J. Jiménez & F. Paulano</i>	121
Fringe projection measurement of highly specular objects in presence of multi-reflection <i>A. Poesch, M. Kaestner & E. Reithmeier</i>	127
Pretreatment and reconstruction of three-dimensional images applied in a locking reconstruction plate for structural analysis with FEA <i>J.P.O. Freitas, E.A.C. Sousa, C.R. Foschini, R.R. Santos & S.C. Rahal</i>	133
Vision-based gesture recognition system for human-computer interaction <i>P. Trigueiros, F. Ribeiro & L.P. Reis</i>	137
A fast and accurate algorithm for detecting and tracking moving hand gestures <i>W.C.S.S. Simões, R. da S. Barboza, V.F. de Lucena Jr. & R.D. Lins</i>	143
Sensor Kinect in a telepresence application <i>A.D.F. Martins, J.M.A. Lourenço, T.R. Patrício & A.R. de Alexandria</i>	151
VIFTrack!—visual-inertial feature tracking based on affine photometric warping <i>D. Aufderheide, W. Krybus & G. Edwards</i>	155
Creation of patient specific finite element models of bone-prosthesis—simulation of the effect of future implants <i>J.J. Ródenas, L. Giovannelli, E. Nadal, J.M. Navarro & M. Tur</i>	161
Direct creation of finite element models from medical images using Cartesian grids <i>L. Giovannelli, O. Marco, J.M. Navarro, E. Giner & J.J. Ródenas</i>	167
An out-of-core volume rendering architecture <i>P.H.J. Amorim, T.F. de Moraes, J.V.L. da Silva & H. Pedrini</i>	173
The Numeric Simulator of Human Body (NSHB)—a future scientific research tool in Medicine <i>P. Ciobanu & S.V. Ciobanu</i>	181
Distribution of the pelvic floor muscle fibers: Comparison between magnetic resonance tractography and finite element method representation <i>S. Brandão, T. Mascarenhas, I. Ramos, M. Parente, T. Roza, R.N. Jorge & H. Ferreira</i>	187
Data quality estimation from interdependencies for structured light scanners <i>M. Krauss, M. Kaestner & E. Reithmeier</i>	191
3D scanning using RGBD imaging devices: A survey <i>E.E.A. Hitomi, J.V.L. da Silva & G.C.S. Ruppert</i>	197
Detection of power lines by image processing <i>P. Seibold, M. Gerke, I. Masár, F. Jelenčiak, P. Bahnik & L. Bahr</i>	203

A study of a firefly meta-heuristics for multithreshold image segmentation <i>H. Erdmann, L.A. Lopes, G.A. Wachs-Lopes, M.P. Ribeiro & P.S. Rodrigues</i>	211
Use of a webcam for movement detection <i>W.R.S. Silva, N.C. Pereti, J.G. Rogeri, A.S. Pereira, N. Marranghello, A.F. Araújo & J.M.R.S. Tavares</i>	219
A computed tomography based orthopedic surgery planning solution <i>J. Ribeiro & V. Alves</i>	223
An intelligent system for polyp detection in wireless capsule endoscopy images <i>I.N. Figueiredo, S. Kumar & P.N. Figueiredo</i>	229
An automatic blood detection algorithm for wireless capsule endoscopy images <i>I.N. Figueiredo, S. Kumar, C. Leal & P.N. Figueiredo</i>	237
Fuzzy reference data estimation in brain tumor segmentation studies <i>E. Binaghi, V. Pedoia, D. Lattanzi, E. Monti, S. Balbi & R. Minotto</i>	243
SVM based pattern recognition of microscopic liver images <i>S. Canale, L. D'Orsi & D. Iacoviello</i>	249
Towards automated image mining from reported medical images <i>N. Gonçalves, G. Vranou & R. Vigário</i>	255
Trends on identification of fractured bone tissue from CT images <i>F. Paulano, J.J. Jiménez & R. Pulido</i>	263
3D shape prior active contours for an automatic segmentation of a patient specific femur from a CT scan <i>D. Almeida, J. Folgado, P.R. Fernandes & R.B. Ruben</i>	271
TV-H ⁻¹ variational inpainting applied to metal artifact reduction in CT images <i>E. Faggiano, T. Lorenzi & S. Perotto</i>	277
An architecture for content-based diagnostic image retrieval in a radiology PACS environment <i>C.A. Berni, J.C.A. Berni & J.A.T.B. da Costa</i>	283
Quantifying the regeneration of bone tissue in biomedical images via Legendre moments <i>J.A. Lachiondo, M. Ujaldón, R. Berretta & P. Moscato</i>	289
CAS tool for DICOM segmentation and analysis <i>P. Teodoro, P. Pires, D. Osório, J. Martins, J.S. da Costa & P. Rego</i>	295
Pattern recognition framework based on the best rank-(R_1, R_2, \dots, R_K) tensor approximation <i>B. Cyganek</i>	301
Classification performance of data mining algorithms applied to breast cancer data <i>V. Santos, N. Datia & M.P.M. Pato</i>	307
Evaluation of the robustness of a CAD method aimed at detecting circumscribed nodules in mammographic images <i>R.R. Rodrigues & L.C. Freire</i>	313
Analysis of pancreas histological images for glucose intolerance identification using ImageJ—preliminary results <i>L.M. Rato, F.C. e Silva, A.R. Costa & C.M. Antunes</i>	319
Classification of microcalcifications on digital mammograms based of FPGA <i>T.A. Dócusse, A.C.R. da Silva, A.S. Pereira & N. Marranghello</i>	323
Fixation procedure for bone reconstruction in maxillo-facial surgery <i>M. Majak, E. Swiatek-Najwer, M. Popek, J. Jaworowski & P. Pietruski</i>	325
Navigated surgical tools calibration issue in computer aided tumor resection procedures <i>M. Popek, E. Swiatek-Najwer, M. Majak, J. Jaworowski & D. Szram</i>	331
Morphometric analysis of the skull shape in children with hydrocephalus <i>D. Larysz, P. Larysz, J. Filipek, W. Wolański, M. Gzik & E. Kawlewska</i>	337

Computer-aided correction of pectus carinatum <i>B. Gzik-Zroska, W. Wolański, E. Kawlewska, M. Gzik, K. Jozzko & J. Dzielicki</i>	341
Preoperative planning the lumbar spine stabilization with posterior intervertebral systems <i>W. Wolański, M. Gzik, E. Kawlewska, E. Stachowiak, D. Larysz, A. Rudnik, I. Krawczyk & P. Bazowski</i>	345
Engineering support for the spine with spondylolisthesis treatment <i>M. Gzik, K. Jozzko & J. Pieniążek</i>	349
Influence of microtomography spatial resolution in mesiovestibular root analysis <i>A.C. Machado, A.S. Machado, R.T. Lopes, I. Lima, B.C. Santos & J.C.M. Oliveira</i>	355
Scanning electron microscope analysis of occlusal rest seats in premolars <i>J.C.R. Campos, A. Correia, M.H. Figueiral, P. Fonseca, F.M. Branco & F. Rodrigues</i>	359
3D finite element analysis of an all-zirconia dental implant rehabilitation <i>A. Correia, J.C.R. Campos, N.V. Ramos, M. Vaz, J.P.C. Viana & Z. Kovacs</i>	361
Bioturbation structures of polychaetes in muddy sediments <i>A.S. Machado, A.C. Machado, K.N. Suzuki, I. Lima, R.T. Lopes & S.F. Pennafirme</i>	365
Visualization of red blood cells flowing through a PDMS microchannel with a microstenosis: An image analysis assessment <i>F.C. Monteiro, B. Taboada & R. Lima</i>	369
Red blood cell motion in experimental micro-circulation and simulations <i>A. João, A. Gambaruto & R. Lima</i>	375
Structural determinants of mechanical behavior of whole human L3 vertebrae—an ex vivo μ CT study <i>Z. Latała, E. Czerwiński, Z. Tabor, R. Petryniak & T. Konopka</i>	377
Mechanical characterization of trabecular bone applied to MRI examinations: In vivo results from 100 patients <i>A. Alberich-Bayarri, W.L. Roque, K. Arcaro & M.A. Pérez</i>	383
An investigation of the mechanical competence parameter to grade the trabecular bone fragility <i>W.L. Roque, K. Arcaro, A. Alberich-Bayarri & Z. Tabor</i>	387
Correlations between fabric tensors computed on cone beam and micro computed tomography images <i>R. Moreno, M. Borga, E. Klintström, T. Brismar & Ö. Smedby</i>	393
Influence of beam hardening artifact in bone interface contact evaluation by 3D X-ray microtomography <i>I. Lima, M. Marquezan, M.M.G. Souza, E.F. Sant'Anna & R.T. Lopes</i>	399
Exploring 3D structure analysis for a simulated remodeling process <i>N. Mellouli & A. Ricordeau</i>	403
Automatic thresholding method for 3D X-ray microtomography analysis <i>E. Sales, W.C.A. Pereira, W. Gómez, I. Lima & R.T. Lopes</i>	409
Influence of mesh size and element type on apparent yield properties of microCT based finite element models of human trabecular bone <i>T. Gross & D.H. Pahr</i>	415
Challenges for bone mineral density calibration on micro-CT <i>R. Stoico, S. Tassani, L. Mecozzi, S. Falcioni, C. Fersini & F. Baruffaldi</i>	419
Trabecular bone: From 2D texture analysis to 3D microarchitecture organization <i>P. Bléry, Y. Amouriq, E. Freuchet, E. Crauste & Jp. Guédon</i>	425
Author index	431

Preface

This book contains invited lectures and full papers presented at VipIMAGE 2013 – IV ECCOMAS Thematic Conference on Computational Vision and Medical Image Processing, which was held in Funchal, Madeira Island, Portugal, during the period 14–16 October 2013. The event had 6 invited lectures, and 74 contributed presentations originated from 17 countries: Austria, Brazil, Canada, Cuba, Czech Republic, Finland, France, Germany, Italy, Poland, Portugal, Republic of Korea, Romania, Spain, Sweden and Venezuela.

Computational methodologies of signal processing and analyses have been commonly used in our society. For instances, full automatic or semi-automatic Computational Vision systems have been increasingly used in surveillance tasks, traffic analysis, recognition process, inspection purposes, human-machine interfaces, 3D vision and deformation analysis.

One of the notable aspects of the Computational Vision domain is the inter- and multi-disciplinarily. Actually, methodologies of more traditional sciences, such as Informatics, Mathematics, Statistics, Psychology, Mechanics and Physics, are regularly comprised in this domain. One of the key motives that contributes for the continually effort done in this field of the human knowledge is the high number of applications that can be easily found in Medicine. For instance, computational algorithms can be applied on medical images for shape reconstruction, motion and deformation analysis, tissue characterization or computer-assisted diagnosis and therapy.

The main objective of these ECCOMAS Thematic Conferences on Computational Vision and Medical Image Processing, initiated in 2007, is to promote a comprehensive forum for discussion on the recent advances in the related fields in order to identify potential collaboration between researchers of different sciences. Henceforth, VipIMAGE 2013 brought together researchers representing fields related to Biomechanics, Biomedical Engineering, Computational Vision, Computer Graphics, Computer Sciences, Computational Mechanics, Electrical Engineering, Mathematics, Statistics, Medical Imaging and Medicine.

The expertises spanned a broad range of techniques for Image Acquisition, Image Processing and Analysis, Signal Processing and Analysis, Data Interpolation, Registration, Acquisition and Compression, Image Segmentation, Tracking and Analysis of Motion, 3D Vision, Computer Simulation, Medical Imaging, Computer Aided Diagnosis, Surgery, Therapy, and Treatment, Computational Bio- imaging and Visualization and Telemedicine, Virtual Reality, Software Development and Applications.

The conference co-chairs would like to take this opportunity to express gratitude for the support given by The International European Community on Computational Methods in Applied Sciences and The Portuguese Association of Theoretical, Applied and Computational Mechanics, and thank to all sponsors, to all members of the Scientific Committee, to all Invited Lecturers, to all Session-Chairs and to all Authors for submitting and sharing their knowledge.

João Manuel R.S. Tavares
Renato M. Natal Jorge
(*Conference co-chairs*)

Acknowledgements

The editors and the Conference co-chairs acknowledge the support towards the publication of the Book of Proceedings and the organization of the IV ECCOMAS Thematic Conference VipIMAGE to the following organizations:

- Universidade do Porto (UP)
- Faculdade de Engenharia da Universidade do Porto (FEUP)
- Instituto de Engenharia Mecânica – Pólo FEUP (IDMEC-Polo FEUP)
- Instituto de Engenharia Mecânica e Gestão Industrial (INEGI)
- European Community on Computational Methods in Applied Sciences (ECCOMAS)
- International Association for Computational Mechanics (IACM)
- Fundação para a Ciência e a Tecnologia (FCT)
- Associação Portuguesa de Mecânica Teórica Aplicada e Computacional (APMTAC)

Invited lecturers

During VipIMAGE 2013, were presented Invited Lectures by 6 Expertises from 3 countries:

- Daniel Cremers, *Technische Universität München, Germany*
- Daniel Rueckert, *Imperial College London, UK*
- Dimitris N. Metaxas, *Rutgers University, USA*
- James S Duncan, *Yale School of Medicine, USA*
- Milan Sonka, *The University of Iowa, USA*
- Richard Bowden, *University of Surrey, UK*

Thematic sessions

Under the auspicious of VipIMAGE 2013, 3 Thematic Sessions were organized:

Imaging of biological flows: Trends and challenges

Alberto Gambaruto, *Instituto Superior Técnico, Portugal*
Mónica S.N. Oliveira, *University of Strathclyde, UK*
Rui Lima, *Polytechnic Institute of Bragança, Portugal*

Trabecular bone characterization: New trends and challenges

Angel Alberich-Bayarri, *Grupo Hospitalario Quirón S.A., Spain*
Waldir L. Roque, *Federal University of Rio Grande do Sul, Brazil*
Fábio Baruffaldi, *Rizzoli Ortopaedic Institut, Italy*
Zbislav Tabor, *Cracow University of Technology, Poland*

Computational vision and image processing applied to dental medicine

André Correia, *Universidade do Porto, Universidade Católica Portuguesa, Portugal*
J.C. Reis Campos, *Universidade do Porto, Portugal*
Mário Vaz, *Universidade do Porto, Portugal*

Scientific committee

All works submitted to VipIMAGE 2013 were evaluated by an International Scientific Committee composed by 84 expert researchers from recognized institutions of 17 countries:

- Ahmed El-Rafei, *Friedrich-Alexander University Erlangen-Nuremberg, Germany*
- Alberto Gambaruto, *Instituto Superior Técnico, Portugal*
- Alejandro F. Frangi, *The University of Sheffield, UK*
- Alexandre Cunha, *California Institute of Technology, USA*
- Ana Mafalda Reis, *University of Porto, Portugal*
- André Correia, *University of Porto, Portugal*
- André R.S. Marçal, *University of Porto, Portugal*
- Andrew D. Bagdanov, *University of Florence, Italy*
- Angel Alberich-Bayarri, *Grupo Hospitalario Quirón S.A., Spain*
- Armando Sousa, *University of Porto, Portugal*
- Arrate Muñoz Barrutia, *Center for Applied Medical Research, Spain*
- Aubrecht Christoph, *AIT Austrian Institute of Technology GmbH, Austria*
- Bernard Gosselin, *Faculte Polytechnique de Mons, Belgium*
- Christos Constantinou, *Stanford University, USA*
- Christos Grecos, *University of West of Scotland, UK*
- Daniela Iacoviello, *Università degli Studi di Roma "La Sapienza", Italy*
- Djemel Ziou, *Universite de Sherbrooke, Canada*
- Durval C. Costa, *Champalimaud Foundation, Portugal*
- Eduardo Borges Pires, *Instituto Superior Técnico, Portugal*
- Eduardo Soudah Prieto, *CIMNE, Spain*
- Emmanuel A. Audenaert, *Ghent University Hospital, Belgium*
- Enrique Alegre Gutiérrez, *University of León, Spain*
- Eugenio Oñate, *Universitat Politècnica de Catalunya, Spain*
- Fábio Baruffaldi, *Rizzoli Ortopaedic Institut, Italy*
- Fernão Abreu, *University of Aveiro, Portugal*
- Filipa Sousa, *University of Porto, Portugal*
- Fiorella Sgallari, *University of Bologna, Italy*
- George Bebis, *University of Nevada, USA*
- Henryk Palus, *Silesian University of Technology, Poland*
- Huiyu Zhou, *Queen's University Belfast, UK*
- Ioannis Pitas, *Aristotle University of Thessaloniki, Greece*
- Isabel M.A.P. Ramos, *University of Porto, Portugal*
- Jaime S. Cardoso, *University of Porto, Portugal*
- Jan C de Munck, *VU University Medical Center, The Netherlands*
- Javier Melenchón, *Universitat Oberta de Catalunya, Spain*
- Jeffrey A. Weiss, *University of Utah, USA*
- Jimmy T. Efird, *East Carolina Heart Institute, USA*
- João M.A. Rebello, *Federal University of Rio de Janeiro, Brazil*
- João Paulo Papa, *São Paulo State University, Brazil*
- João Paulo Vilas-Boas, *University of Porto, Portugal*
- Joaquim Silva Gomes, *University of Porto, Portugal*
- Jordi González, *Centre de Visió per Computador, Spain*
- Jorge M.G. Barbosa, *University of Porto, Portugal*
- Jorge S. Marques, *Instituto Superior Técnico, Portugal*
- José C. Reis Campos, *University of Porto, Portugal*

- Jose M. García Aznar, *University of Zaragoza, Spain*
- Khan M. Iftekharuddin, *The University of Memphis, USA*
- Kristian Sandberg, *Computational Solutions, USA*
- Laurent Cohen, *Universite Paris Dauphine, France*
- Lionel Moisan, *Université Paris V, France*
- Luís Amaral, *Polytechnic Institute of Coimbra, Portugal*
- Luís Paulo Reis, *University of Minho, Portugal*
- Lyuba Alboul, *Sheffield Hallam University, UK*
- M. Emre Celebi, *Louisiana State University in Shreveport, USA*
- Mahmoud El-Sakka, *The University of Western Ontario, Canada*
- Manuel Filipe Costa, *University of Minho, Portugal*
- Manuel González Hidalgo, *University of the Balearic Islands, Spain*
- Manuel Ujaldon, *University of Malaga, Spain*
- Manuele Bicego, *University of Verona, Italy*
- Marc Thiriet, *Universite Pierre et Marie Curie, France*
- Marcos Rodrigues, *Sheffield Hallam University, UK*
- Mário Forjaz Secca, *Universidade Nova de Lisboa, Portugal*
- Mário Vaz, *University of Porto, Portugal*
- Miguel Velhote Correia, *University of Porto, Portugal*
- Mislav Grgic, *University of Zagreb, Croatia*
- Mónica N.S. Oliveira, *University of Strathclyde, UK*
- Nguyen Dang Binh, *Hue University, Vietnam*
- Nuno Machado, *Polytechnic Institute of Lisbon, Portugal*
- Paulo Flores, *University of Minho, Portugal*
- Pedro Almeida, *University of Lisbon, Portugal*
- Philippe G. Young, *University of Exeter, UK*
- Rainald Lohner, *George Mason University, USA*
- Reneta Barneva, *State University of New York at Fredonia, USA*
- Rui Lima, *Polytechnic Institute of Bragança, Portugal*
- Sabina Tangaro, *Instituto Nazionale di Fisica Nucleare, Italy*
- Slimane Larabi, *USTHB University, Algeria*
- Susana Branco Silva, *Polytechnic Institute of Lisbon, Portugal*
- Teresa Mascarenhas, *University of Porto, Portugal*
- Thierry Brouard, *University of Tours, France*
- Tolga Tasdizen, *University of Utah, USA*
- Waldir L. Roque, *Federal University of Rio Grande do Sul, Brazil*
- Yongjie (Jessica) Zhang, *Carnegie Mellon University, USA*
- Zbislav Tabor, *Cracow University of Technology, Poland*
- Zeyun Yu, *University of Wisconsin at Milwaukee, USA*

Invited lectures

Machine learning meets medical imaging: Learning and discovery of clinically useful information from images

Daniel Rueckert & Robin Wolz

Biomedical Image Analysis Group, Department of Computing, Imperial College London, UK

Paul Aljabar

Department of Biomedical Engineering, Division of Imaging Sciences and Biomedical Engineering, King's College London, UK

ABSTRACT: Three-dimensional (3D) and four-dimensional (4D) imaging plays an increasingly important role in computer-assisted diagnosis, intervention and therapy. However, in many cases the interpretation of these images is heavily dependent on the subjective assessment of the imaging data by clinicians. Over the last decades image registration has transformed the clinical workflow in many areas of medical imaging. At the same time, advances in machine learning have transformed many of the classical problems in computer vision into machine learning problems. This paper will focus on the convergence of image registration and machine learning techniques for the discovery and quantification of clinically useful information from medical images. We will illustrate this with several examples such as the segmentation of neuro-anatomical structures, the discovery of biomarkers for neurodegenerative diseases and the quantification of temporal changes such as atrophy in Alzheimer's disease.

1 INTRODUCTION

For many clinical applications the analysis of medical images represents an important aspect in decision making in the context of diagnosis, treatment planning and therapy. Different imaging modalities often provide complementary anatomical information about the underlying tissues such as the X-ray attenuation coefficients from X-ray computed tomography (CT), and proton density or proton relaxation times from magnetic resonance (MR) imaging. Medical images allow clinicians to gather information about the size, shape and spatial relationship between anatomical structures and any pathology, if present. In addition to CT and MR, other imaging modalities provide functional information such as the blood flow or glucose metabolism from positron emission tomography (PET) or single-photon emission tomography (SPECT), and permit clinicians to study the relationship between anatomy and physiology. Finally, histological images provide another important source of information which depicts structures at a microscopic-level of resolution.

The use of machine learning in the analysis of medical images has become increasingly important in many real-world, clinical applications ranging from the acquisition of images of moving organs

such as the heart, liver and lungs to the computer-aided detection, diagnosis and therapy. For example, machine learning techniques such as clustering can be used to identify classes in the image data and classifiers may be used to differentiate clinical groups across images or tissue types within an image. These techniques may be applied to images at different levels: At the lowest level or voxel level one may be interested in classifying the voxel as part of a tissue class such as white matter or grey matter. At a more intermediate level, classification may be applied to some representation or features extracted from the images. For example, one may be interested in classifying the shape of the hippocampus as belonging to a healthy control or to a subject with dementia. At the highest level, clustering may be applied in order to classify entire images.

In the following we will discuss two particular applications of image registration and machine learning in medical imaging: (a) segmentation and (b) biomarker discovery and classification.

2 MACHINE LEARNING FOR SEGMENTATION

The amount of data produced by imaging increasingly exceeds the capacity for expert visual

analysis, resulting in a growing need for automated image analysis. In particular, accurate and reliable methods for segmentation (classifying image regions) are a key requirement for the extraction of information from images. In recent years many approaches to image segmentation have emerged that use image registration as a key component. Many of these approaches are based on so-called *atlases*. An atlas can be viewed as a map or chart of the anatomy or function, either from a single individual or from an entire population. In many cases the atlases are annotated to include geometric information about points, curves or surfaces, or label information about voxels (anatomical regions or function). Such atlases are often used in brain imaging applications (Mazziotta, Toga, Evans, Fox, & Lancaster 1995).

Atlases can be used as prior information for image segmentation. In general, an atlas A can be viewed as a mapping from a set of spatial coordinates (i.e. the voxels) to a set of labels $\Lambda = \{1, \dots, L\}$. By warping the atlas to the target, one can make the atlas and its prior information *subject-specific* and obtain a segmentation L of image I :

$$L = A \circ \mathbf{T}_{A \rightarrow I} \quad (1)$$

Here $\mathbf{T}_{A \rightarrow I}$ denotes the transformation that maps the atlas A into the space of the image I . This transformation can be obtained using different image registration techniques, e.g. (Rueckert, Sonoda, Hayes, Hill, Leach, & Hawkes 1999).

Indeed the earliest approaches to segmentation via registration have used such approaches: By registering a labelled atlas to the target images and transforming the segmentation of the atlas into the coordinate system of the subject one can obtain a segmentation of the subject's image (Miller, Christensen, Amit, & Grenander 1993, Collins & Evans 1997). This segmentation approach is simple yet effective since the approach can segment any of the structures that are present and annotated in the atlas. However, the accuracy and robustness of the segmentation is dictated by the accuracy and robustness of the image registration. Errors in the registration process will directly affect the accuracy of the propagated segmentation.

2.1 Multi-atlas segmentation

In the area of machine learning it is well known that the performance of pattern recognition techniques can be boosted using combining classifiers (Kittler, Hatef, Duin, & Matas 1998). This concept can be exploited in the context of atlas-based segmentation: Assuming the availability of multiple atlases, the output of atlas-based segmentation using a

particular atlas instance can be viewed the output of the classifier. Combining the output of multiple classifiers (or segmentations) into a single consensus segmentation has been shown to reduce random errors in the individual atlas-to-image registration resulting in an improved segmentation (Rohlfing & Maurer Jr. 2005, Heckemann, Hajnal, Aljabar, Rueckert, & Hammers 2006). Using this method each atlas is registered to the target image in question. The resulting transformation is then used to transform the segmentation from the atlas into the coordinate system of the target image.

By applying classifier fusion techniques at every voxel in subject space the final consensus segmentation can be applied. Several classifier fusion techniques can be used, see (Kittler, Hatef, Duin, & Matas 1998) for a detailed review and discussion of the different classifier fusion techniques. One of the most popular techniques is the majority vote rule (Rohlfing & Maurer Jr. 2005): It simply uses a *winner-takes-all* approach in which each voxel is assigned the label that gets the most votes from the individual segmentations. Assuming K classifiers (i.e. atlases) final segmentation $L(\mathbf{p})$ can be expressed as

$$L(\mathbf{p}) = \max[f_1(\mathbf{p}), \dots, f_L(\mathbf{p})] \quad (2)$$

where

$$f_l(\mathbf{p}) = \sum_{k=1}^K w_{k,l}(\mathbf{p}) \quad \text{for } l=1, \dots, L \quad (3)$$

and

$$w_{k,l}(\mathbf{p}) = \begin{cases} 1, & \text{if } l = e_k(\mathbf{p}) \\ 0, & \text{otherwise} \end{cases} \quad (4)$$

Here e_k denotes the output or label of classifier k . An extension of multi-atlas segmentation has been proposed in (Aljabar, Heckemann, Hammers, Hajnal, & Rueckert 2009). In their work a large number of atlases are used. However, instead of using all atlases for multi-atlas segmentation, only the most similar atlases are used: In the first step all atlases are registered to a common standard space using a coarse registration (e.g. affine registration). In addition, the target image is also aligned to the common standard space. After this initial alignment the similarity between each atlas and the target image can be determined using an image similarity measure S , e.g. sums of squared differences (SSD), cross-correlation (CC), mutual information (MI) (Collins, Evans, Holmes, & Peters 1995, Viola & Wells 1995) or normalised mutual information (NMI) (Studholme, Constable,

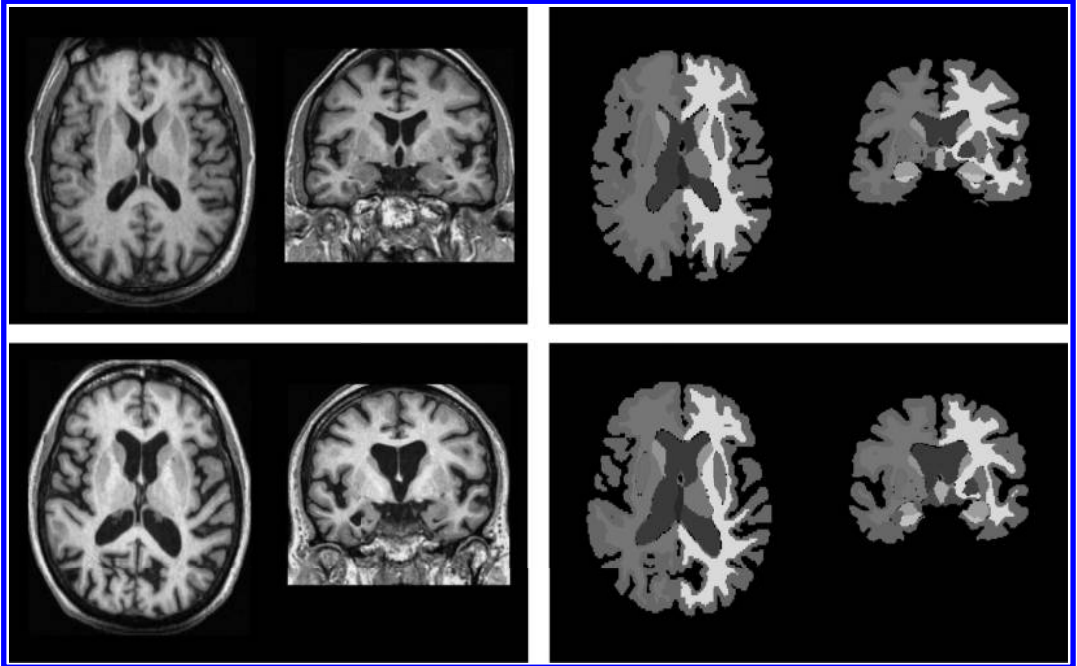


Figure 1. Result of multi-atlas segmentation of brain MR images from a normal control subject (top) and subject with Alzheimer's disease (bottom).

& Duncan 1999). This allows the ranking of all atlases with respect to the similarity to the target image. The m top-ranked atlases are then registered non-rigidly to the target image and as before a classifier fusion framework is applied to obtain a final consensus segmentation.

The use of a common standard space allows the pre-registration of all atlases to the standard common space avoiding the necessity for performing registration of each atlas to the target image for atlas selection. In principle it is also possible to rank atlases based on meta-information available from the atlases and the target image. Such meta-information can include gender, age, handedness and clinical status. In this case atlas selection can be carried out independently from the actual image data and does not require any initial registration for the atlas selections step.

Instead of ranking atlases based on their similarity to the target image and using the top m atlases for classifier fusion, it is possible to weight each atlas according to its similarity to the target image. In this case the weight w can be written as

$$w_{k,l}(\mathbf{p}) = \begin{cases} S, & \text{if } l = e_k(\mathbf{p}) \\ 0, & \text{otherwise} \end{cases} \quad (5)$$

where S measures the similarity between atlas A_k and the target image. It should be noted that the atlas selection scheme can be viewed as a special case of the weighted atlas fusion scheme described above where $w = 1$ for the top-ranked atlases and $w = 0$ for all other atlases.

While weighted voting allows the incorporation of a notation of atlas similarity into the classifier fusion, it does not account for the fact that images can be dissimilar at a global level but similar at a local level and vice versa. For example, two brain MR images may have ventricles that are very different in size and shape but their hippocampi may have similar shape and size. Since the ventricle is much larger than the hippocampus, its appearance will dominate the similarity calculations. A more flexible approach is to measure image similarity locally and to adjust the weighting function accordingly:

$$w_{k,l}(\mathbf{p}) = \begin{cases} S(\mathbf{p}), & \text{if } l = e_k(\mathbf{p}) \\ 0, & \text{otherwise} \end{cases} \quad (6)$$

Another approach is based on simultaneous truth and performance level estimation (STAPLE) (Warfield, Zhou, & Wells 2004). The STAPLE framework was initially created in order to

fuse several manual or automated segmentations of the same image. More specifically it computes a probabilistic estimate of the true segmentation as a measure of the performance level represented by each segmentation in an expectation-maximization (EM) framework. This framework has extended to account for spatially varying performance by extending the performance level parameters to account for a smooth, voxelwise performance level field that is unique to each atlas-based segmentation (Commowick, Akhondi-Asl, & Warfield 2012, Asman & Landman 2012).

3 MACHINE LEARNING FOR BIOMARKER DISCOVERY AND CLASSIFICATION

A biomarker is a measurement or physical sign used as a substitute for a clinically meaningful endpoint that measures directly how a patient feels, functions, or survives. Changes induced by a therapy on a surrogate endpoint are expected to reflect changes on a clinically meaningful endpoint. A practical example of a biomarker could be the volume of region of interest (ROI) such as the hippocampus. However, this requires a-priori information about what anatomical ROI maybe affected by a particular disease. An alternative approach is to learn the biomarker directly from the images without any a-priori knowledge.

One of the key challenges in applying machine learning techniques for biomarker discovery in medical images is the fact that medical images are often represented as data points in a very high-dimensional space, yet they only occupy a small part of this space. Another key challenge that is often faced is commonly referred to as the small sample size problem: While the data lives in a very high-dimensional space we often only have a comparatively small number of images from which to learn. In this context manifold learning techniques (Aljabar, Wolz, & Rueckert 2012) offer a powerful approach to find a representation of images or image-derived features that facilitates the application of machine learning techniques such as clustering or regression.

The basic idea of manifold learning is closely related to that of dimensionality reduction techniques such as Principal Component Analysis (PCA). The key assumption in applying manifold learning techniques is that dimensionality of the original data can be reduced with a negligible loss of information. For example, a 3D brain image with $256 \times 256 \times 128$ voxels may be viewed as a point in a more than 8 million dimensional vector space. However, brain images from different subjects have a large degree of similarity in their appearance. Thus, most regions of this high-dimensional space

correspond to images that have no similarity to brain images. Instead the assumption is that the images are data points on a low dimensional manifold, which is embedded in the high-dimensional space. The goal of manifold learning algorithms is to uncover or learn this low dimensional manifold directly from the data.

A good example of the application of manifold learning to biomarker discovery can be found in (Wolz, Aljabar, Hajnal, & Rueckert 2010): In their work, the MR brain images from a population of subjects with and without Alzheimer's disease were analysed using a manifold learning approach based on Laplacian eigenmaps (Belkin & Niyogi 2003):: The set of images $\{\mathbf{x}_1, \dots, \mathbf{x}_n\}$ is described by N images $\mathbf{x}_i \in R$, each being defined as a vector of intensities, where D is the number of voxels per image or region of interest. Assuming that $\{\mathbf{x}_1, \dots, \mathbf{x}_n\}$ lie on or near a d -dimensional manifold M embedded in R^D and $d \ll D$, it is possible to learn a new, low dimensional representation $\{\mathbf{y}_1, \dots, \mathbf{y}_n\}$ with $\mathbf{y}_i \in R$, of the input images. In Laplacian eigenmaps a set of weights w_{ij} are defined as the similarities between images within a local neighborhood and are set to zero for all other pairings. Similarities can be derived from distances d_{ij} using a heat kernel such as

$$w_{ij} = e^{-\frac{d_{ij}^2}{t}} \quad (7)$$

where t defines the width of the kernel. The Laplacian eigenmap embedding is obtained by minimizing the objective function

$$\phi(\mathbf{Y}) = \sum_{ij} \|\mathbf{y}_i - \mathbf{y}_j\|^2 w_{ij} = 2\mathbf{Y}^T \mathbf{L} \mathbf{Y} \quad (8)$$

where $\mathbf{L} = \mathbf{D} \mathbf{W}$ is the graph Laplacian matrix which is derived from the weight matrix \mathbf{W} and the diagonal degree matrix \mathbf{D} where $\mathbf{D}_{ii} = \sum_j w_{ij}$. The Laplacian eigenmap objective function is optimized under the constraint that $\mathbf{y}^T \mathbf{D} \mathbf{y} = 1$ which removes an arbitrary scaling factor in the embedding and prevents the trivial solution where all \mathbf{y}_i are zero. The \mathbf{y}_i that optimize the objective function are defined by the eigenvectors corresponding to the smallest nonzero eigenvalues of the generalized eigenvalue problem $\mathbf{L} \mathbf{v} = \lambda \mathbf{D} \mathbf{v}$.

An example of a manifold constructed from brain MR images using Laplacian eigenmaps is shown in Figure 2: In this example a set of baseline and follow-up MR images from the ADNI study have been embedded into a two-dimensional manifold. In this manifold each pair of baseline and follow-up images correspond to a pair of points in the manifold connected by a line. The line indicates the magnitude and direction of movement of

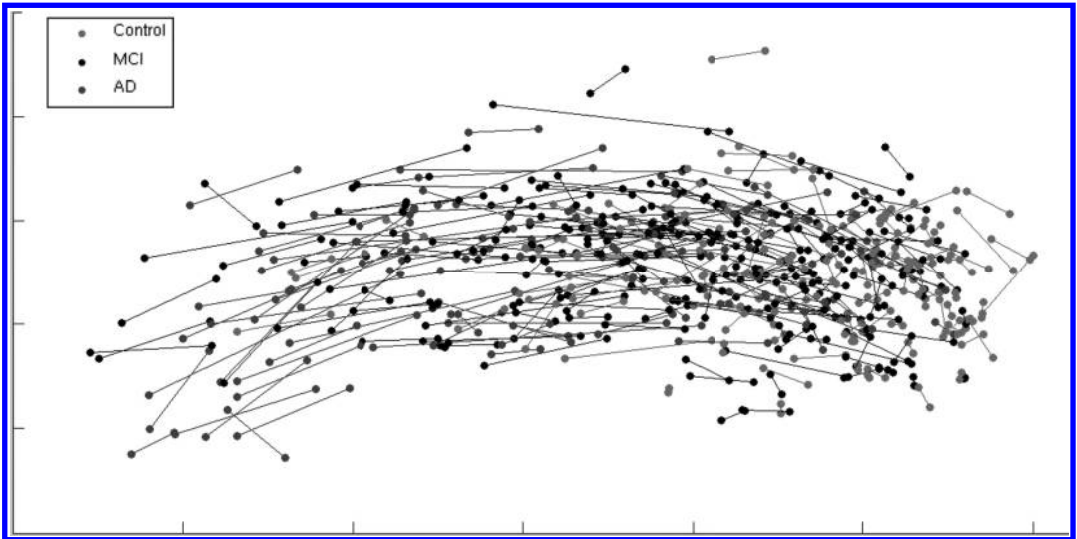


Figure 2. Example of manifold learning for biomarker discovery and classification (Wolz, Aljabar, Hajnal, & Rueckert 2010): A set of baseline and follow-up MR images from the ADNI study is embedded into a two-dimensional manifold: The figure clearly shows the difference in the longitudinal trajectory between healthy controls and subjects with AD.

each subject between baseline and follow-up (in this case 24 months after baseline). Using the position, magnitude and direction of movement in the manifold as features for a linear SVM it is possible to achieve classification rates of up-to 86% for the classification of controls and subjects with AD (Wolz, Aljabar, Hajnal, & Rueckert 2010).

4 SUMMARY AND CONCLUSIONS

Machine learning is becoming increasingly important in the context of medical imaging. In this article we have described two different exemplar applications of machine learning for image segmentation and biomarker discovery/classification. There are many more potential applications for machine learning in this area. However, one of the challenges is that the application of machine learning usually requires a large number of training datasets. In medical imaging it is often very costly and time-consuming to acquire such large number of training datasets. In future this challenge may be overcome as shared data repositories become more widely available.

REFERENCES

- Aljabar, P., R. Heckemann, A. Hammers, J. Hajnal, & D. Rueckert (2009). *Multi-atlas based segmentation of brain images: Atlas selection and its effect on accuracy*. *NeuroImage* 46(3), 726–738.
- Aljabar, P., R. Wolz, & D. Rueckert (2012). Manifold learning for medical image registration, segmentation and classification. In K. Suzuki (Ed.), *Machine Learning in Computer Aided Diagnosis*. Igi.
- Asman, A. & B.A. Landman (2012). Formulating spatially varying performance in the statistical fusion framework. *IEEE Transactions on Medical Imaging* 31(6), 1326–1336.
- Belkin, M. & P. Niyogi (2003). Laplacian eigenmaps for dimensionality reduction and data representation. *Neural Computation* 15(6), 1373–1396.
- Collins, D.L. & A.C. Evans (1997). Animal: validation and applications of non-linear registration-based segmentation. *International Journal of Pattern Recognition and Artificial Intelligence* 11, 1271–1294.
- Collins, D.L., A.C. Evans, C. Holmes, & T.M. Peters (1995). Automatic 3D segmentation of neuro-anatomical structures from MRI. In *Information Processing in Medical Imaging: Proc. 14th International Conference (IPMI'95)*, pp. 139–152.
- Commowick, O., A. Akhondi-Asl, & S.K. Warfield (2012). Estimating a reference standard segmentation with spatially varying performance parameters: local map staple. *IEEE Transactions on Medical Imaging* 31(8), 1593–1606.
- Heckemann, R.A., J.V. Hajnal, P. Aljabar, D. Rueckert, & A. Hammers (2006). Automatic anatomical brain mri segmentation combining label propagation and decision fusion. *Neuroimage* 33(1), 115–126.
- Kittler, J., M. Hatef, R.P.W. Duin, & J. Matas (1998). On combining classifiers. *IEEE Transactions on Pattern Analysis and Machine Intelligence* 20(3), 226–239.
- Mazziotta, J., A. Toga, A. Evans, P. Fox, & J. Lancaster (1995). A probabilistic atlas of the human brain: Theory and rationale for its development. *The*

- International Consortium for Brain Mapping. NeuroImage* 2(2), 89–101.
- Miller, M., G.E. Christensen, Y. Amit, & U. Grenander (1993). Mathematical textbook of deformable neuro-anatomies. In *Proc. Natl. Acad. Sci. USA, Volume 90*, pp. 11944–11948.
- Rohlfing, T. & C.R. Maurer Jr. (2005). Multi-classifier framework for atlas-based image segmentation. *Pattern Recognition Letters* 26(13), 2070–2079.
- Rueckert, D., L.I. Sonoda, C. Hayes, D.L.G. Hill, M.O. Leach, & D.J. Hawkes (1999). Non-rigid registration using freeform deformations: Application to breast MR images. *IEEE Transactions on Medical Imaging* 18(8), 712–721.
- Studholme, C., R.T. Constable, & J.S. Duncan (1999). Incorporating an image distortion model in non-rigid alignment of EPI with conventional MRI. In *Information Processing in Medical Imaging: Proc. 16th International Conference (IPMI'99)*, pp. 454–459.
- Viola, P. & W.M. Wells (1995). Alignment by maximization of mutual information. In *Proc. 5th International Conference on Computer Vision (ICCV'95)*, pp. 16–23.
- Warfield, S.K., K.H. Zhou, & W.M. Wells (2004). Simultaneous truth and performance level estimation (STAPLE): An algorithm for the validation of image segmentation. *IEEE Transactions on Medical Imaging* 23(7), 903–921.
- Wolz, R., P. Aljabar, J. Hajnal, & D. Rueckert (2010). Manifold learning for biomarker discovery. In *Workshop on Machine Learning in Medical Imaging (MLMI)*, pp. 116–123.